

Supporting Information

An Oligothiophene Chromophore with a Macrocyclic Side Chain: Synthesis, Morphology, Charge Transport, and Photovoltaic Performance

Swaminathan Venkatesan,^a Jianyuan Sun,^a Lianjie Zhang,^{a,e} Ashish Dubey,^b Andrew Sykes,^c Ting-Yu Lin,^d Yu-Chueh Hung,^d Qiquan Qiao^b and Cheng Zhang^{a*}

^a Department of Chemistry and Biochemistry, South Dakota State University, SD, USA

^b Department of Electrical Engineering, South Dakota State University, SD, USA

^c Department of Chemistry, University of South Dakota, Vermillion, SD57069

^d Institute of Photonics Technologies, National Tsing Hua University, Taiwan

^e Current address: Institute of Polymer Optoelectronic Materials & Devices, South China University of Technology, Guangzhou 510640, People's Republic of China

cheng.zhang@sdstate.edu

Table of Contents

Figure S1-10. ¹H and ¹³C NMR spectrum of synthesized compounds.

Figure S11. The unit cell of RingBDT(T₃CHO)₂ and the side and top views of the molecule.

Figure S12. RingBDT(T₃CHO)₂ dimer in single crystal.

Figure S13. The side, top and end views of two sets of stacked RingBDT(T₃CHO)₂ dimers.

Figure S14. A four-cycle DSC scan of RingBDT(T₃A).

Figure S15. A four-cycle DSC scan of RingBDT(T₃A) at a heating and cooling rate of 20 °C/min.

Figure S16. DSC thermograms of four chromophores.

Figure S17. X-ray diffractogram of RingBDT(T₃A)₂ particles.

Figure S18. Optical images of BDT(T₃A)₂ and RingBDT(T₃A)₂ films.

Figure S19. UV-vis absorption spectra of RingBDT(T₃A)₂ CHCl₃ solutions of different concentrations.

Figure S20. UV-vis absorption spectra of BDT(T₃A)₂ chloroform solutions of different concentrations.

Figure S21. Cyclic voltammograms of RingBDT(T₃A)₂ and BDT(T₃A)₂ films over a wide potential range (-2 V to +2 V).

Figure S22. Cyclic voltammograms of RingBDT(T₃A)₂ (a) and BDT(T₃A)₂ (b) thicker films.

Figure S23. Cyclic voltammograms of RingBDT(T₃A)₂ and BDT(T₃A)₂ solutions.

Table S1. Performance of inverted solar cells of BDT(T₃A)₂: PC₆₀BM (as deposited)

Table S2. Performance of inverted solar cells of BDT(T₃A)₂: PC₆₀BM annealed at 100 °C for 10 minutes.

Table S3. Performance of inverted solar cells of RingBDT(T₃A)₂: PC₆₀BM (as deposited, no DIO)

Table S4. Performance of inverted solar cells of RingBDT(T₃A)₂: PC₆₀BM (as deposited, with DIO)

Table S5. Performance of inverted solar cells of RingBDT(T₃A)₂: PC₆₀BM (with DIO, and annealed)

Table S6. RingBDT(T₃A)₂ devices performances of devices in a normal device configuration.

Table S7. BDT(T₃A)₂ devices performances of devices in a normal device configuration.

Figure S24. The absorption spectra of RingBDT(T₃A)₂: PC₆₀BM films processed without and with DIO.

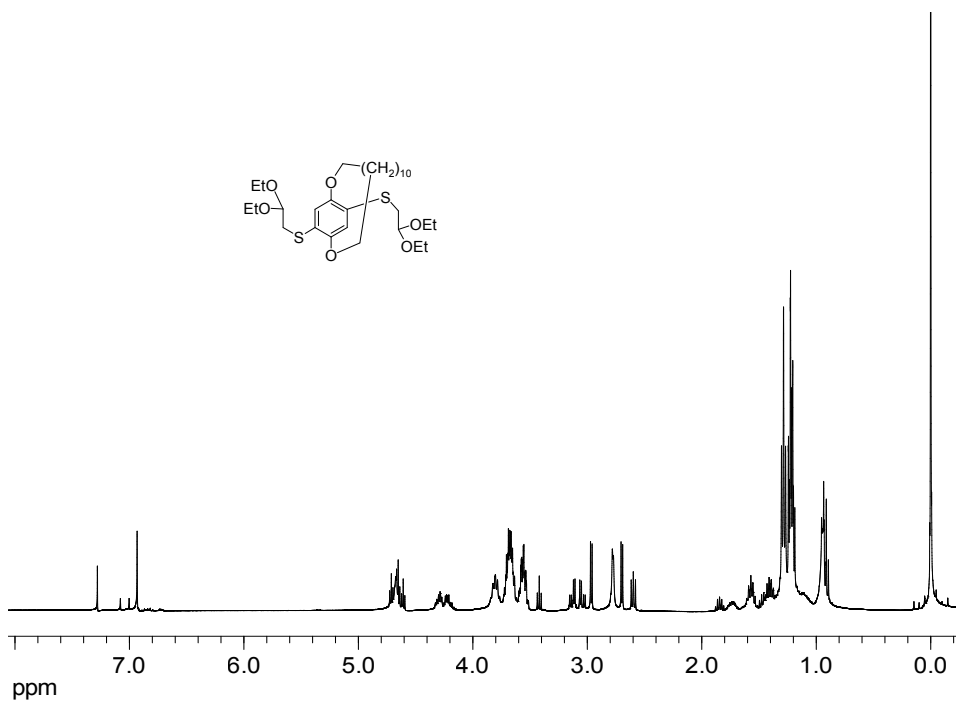


Figure S1. ¹H NMR spectrum of compound 3.

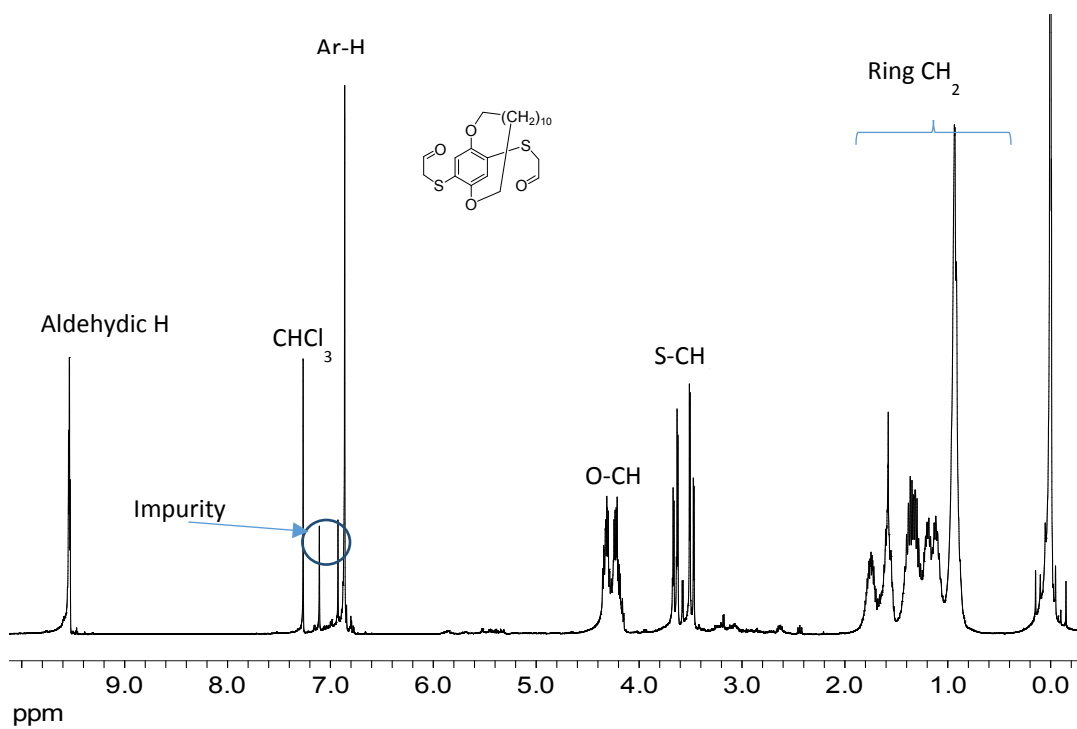


Figure S2. ¹H NMR spectrum of compound 4.

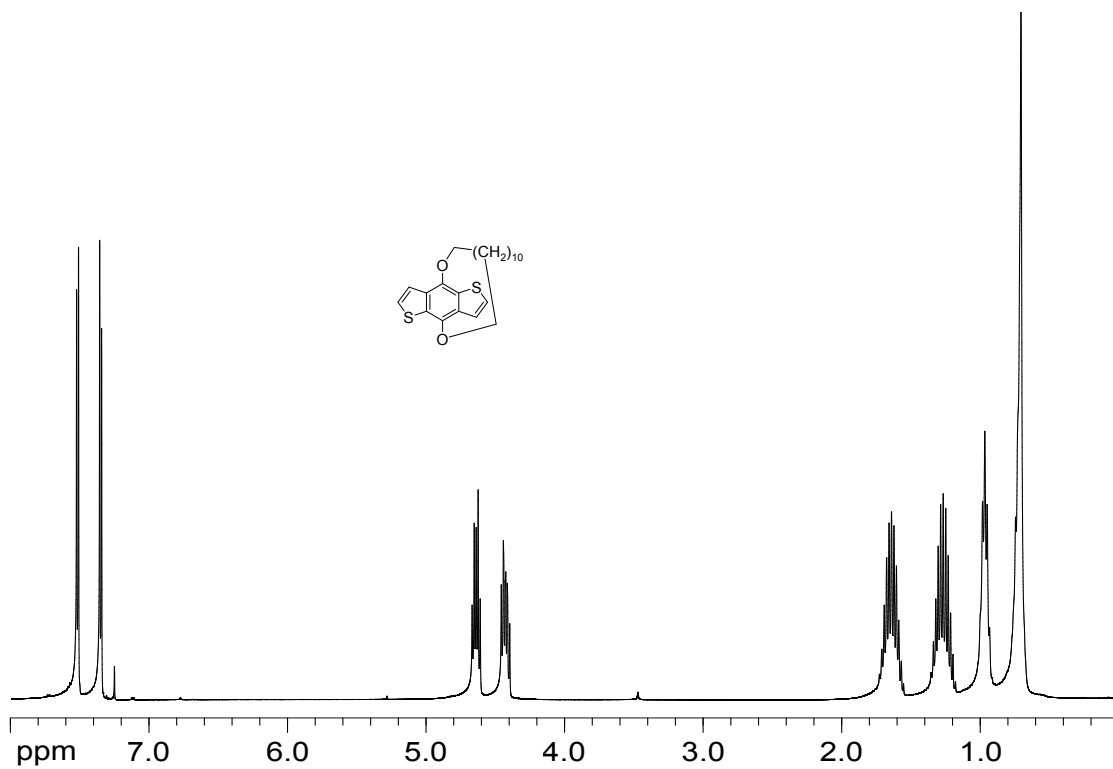


Figure S3. ¹H NMR spectrum of compound 5.

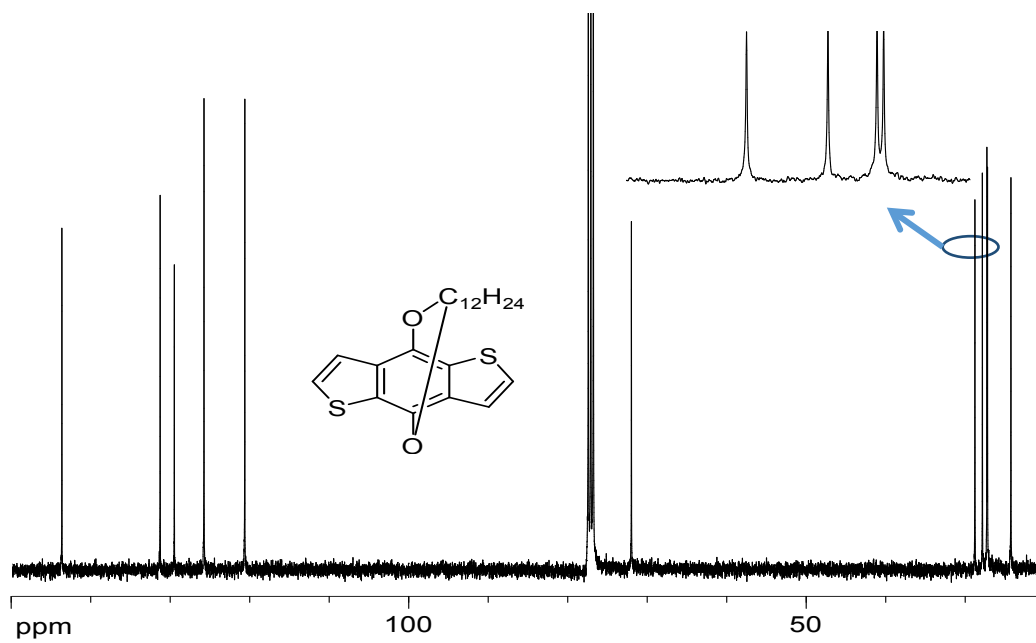


Figure S4. ¹³C NMR spectrum of compound 5.

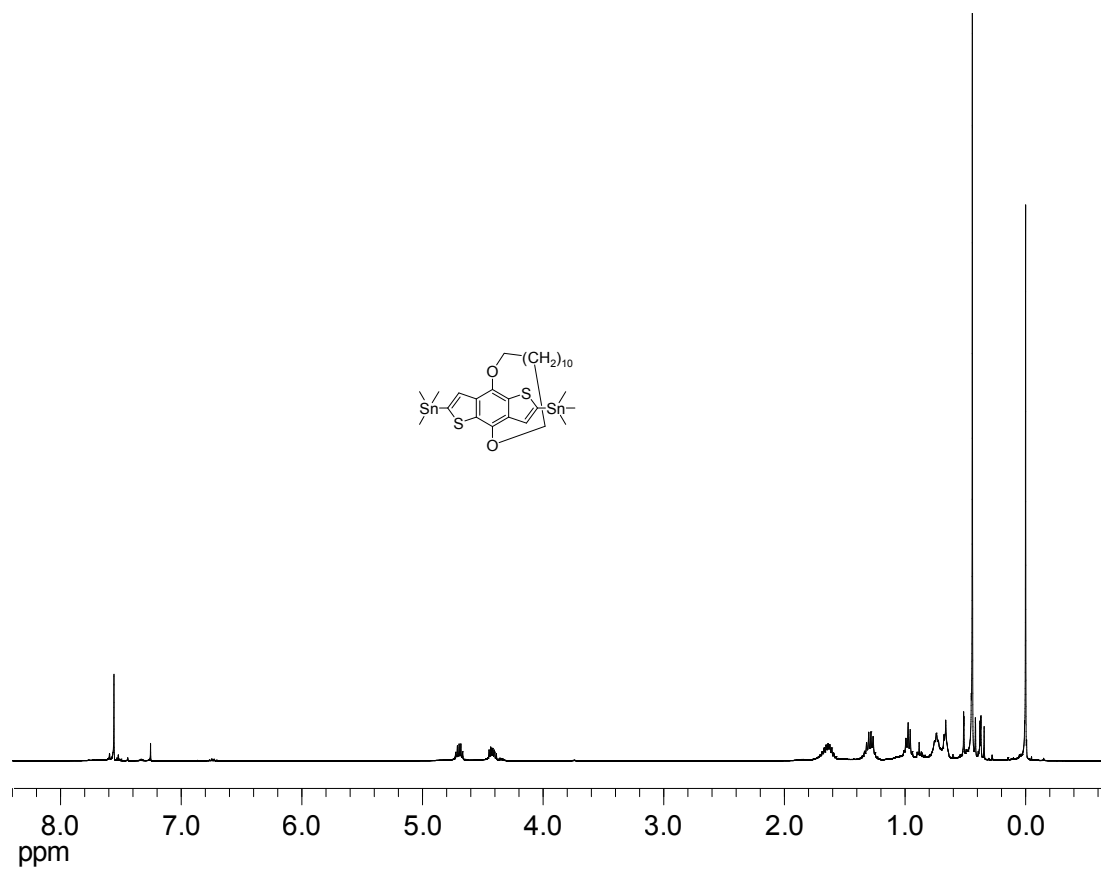


Figure S5. ¹H NMR spectrum of compound 6.

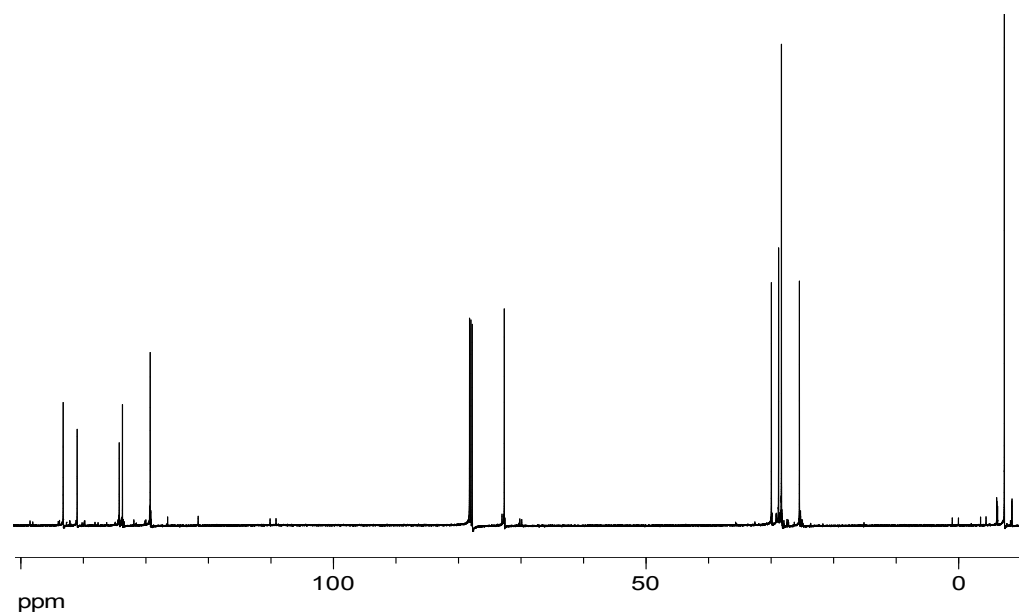


Figure S6. ¹³C NMR spectrum of compound 6.

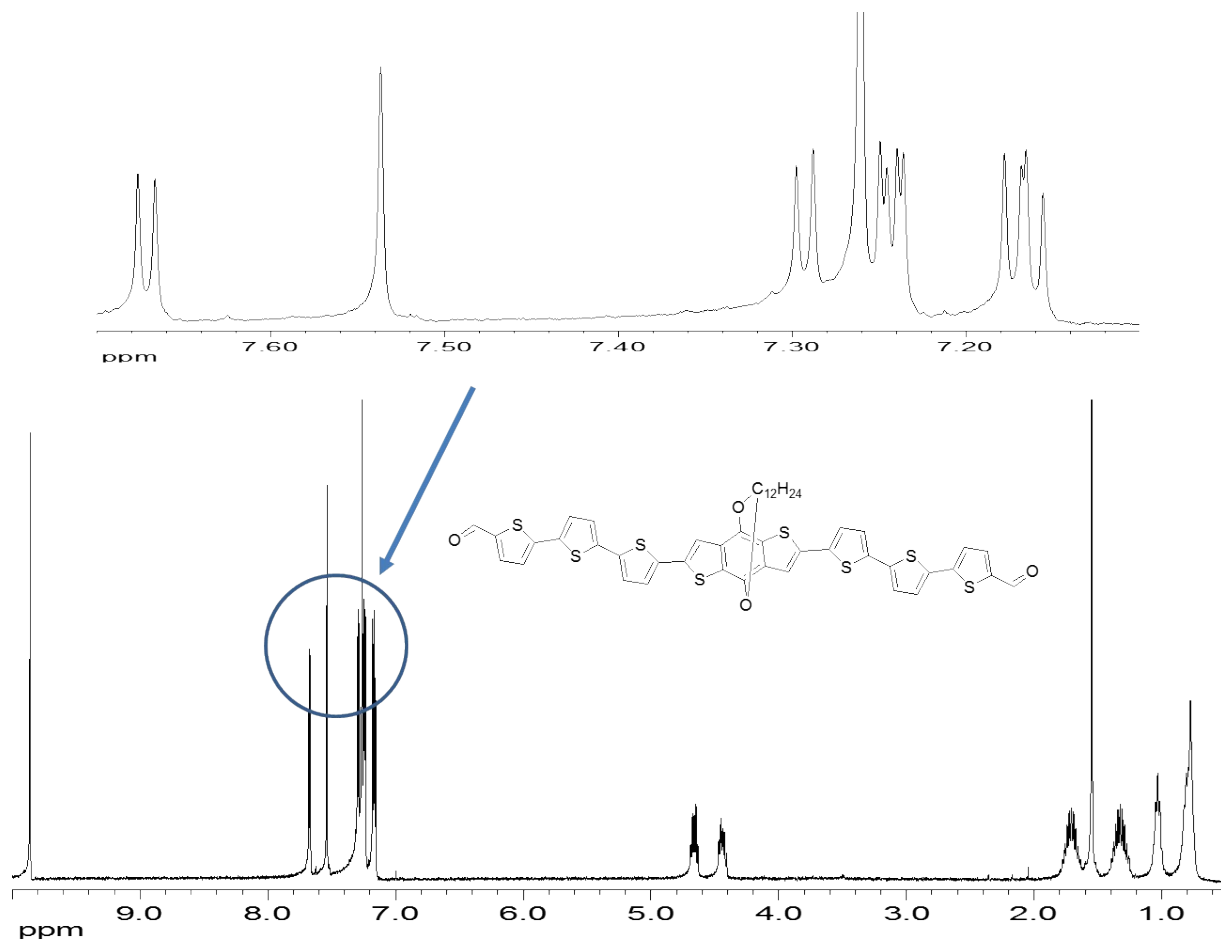
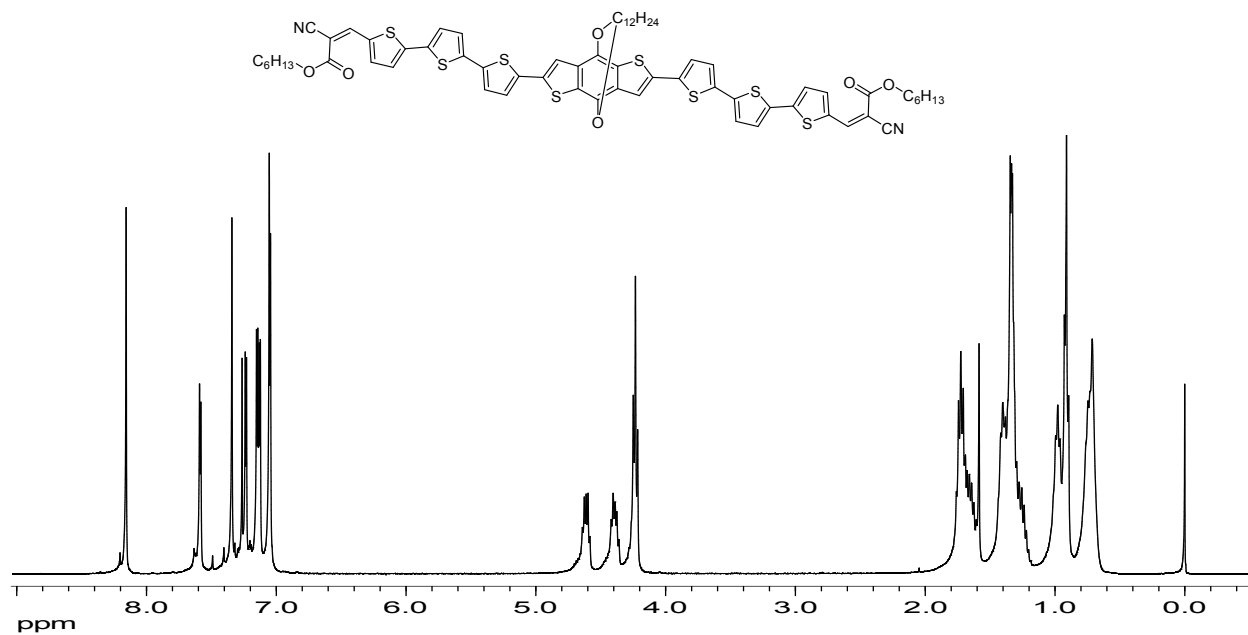


Figure S7. ^1H NMR spectrum of RingBDT(T_3CHO) $_2$.



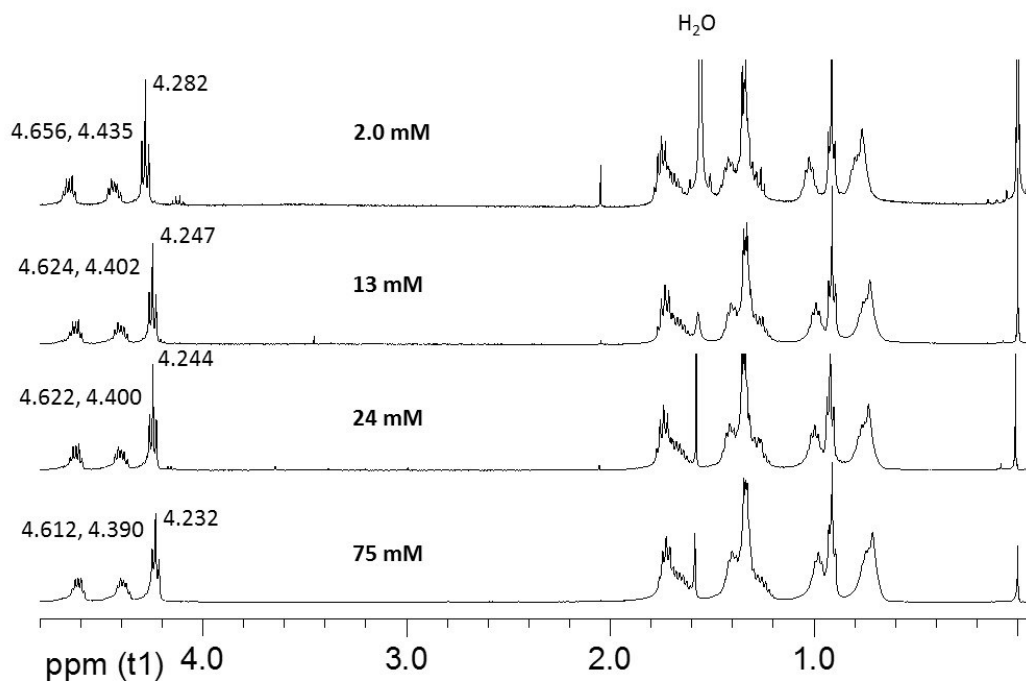


Figure S8. ^1H NMR spectrum of RingBDT(T_3A) $_2$: full spectrum (top) and spectra of the aliphatic region at different chromophore concentrations.

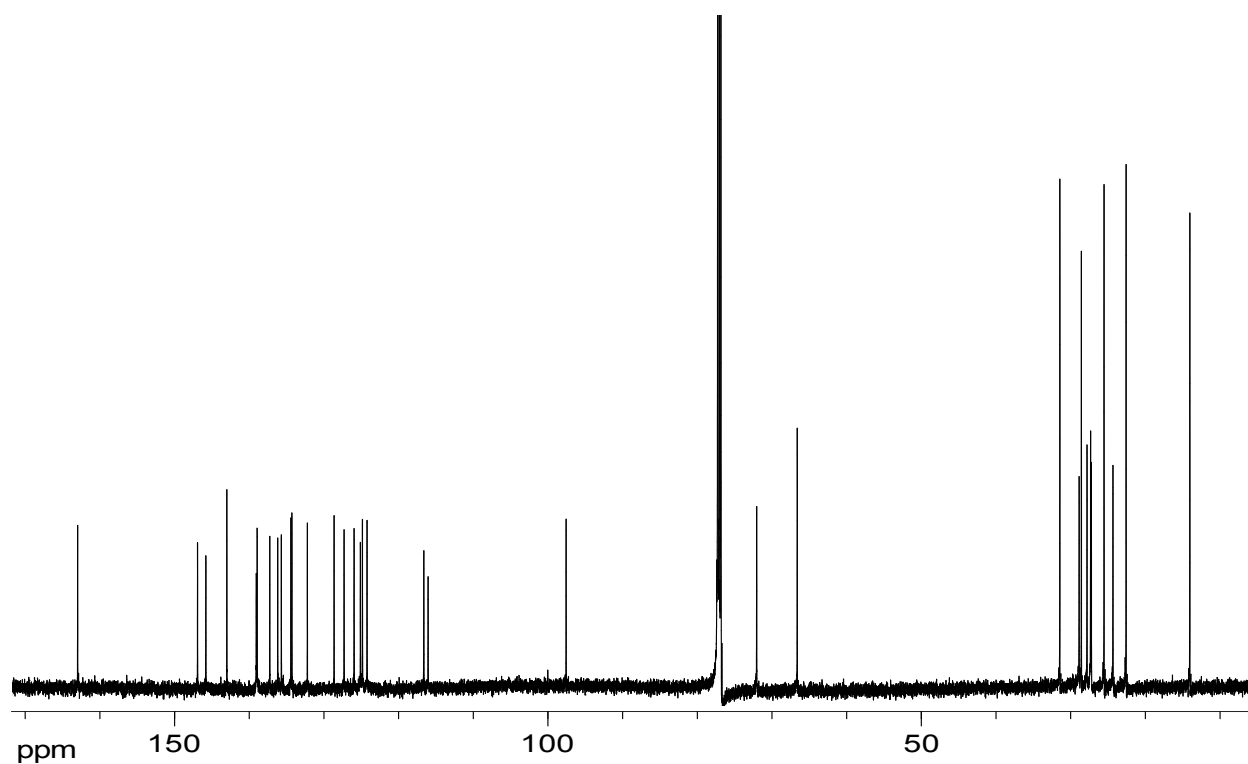


Figure S9. ^1H NMR spectrum of RingBDT(T_3A) $_2$ (600 MHz).

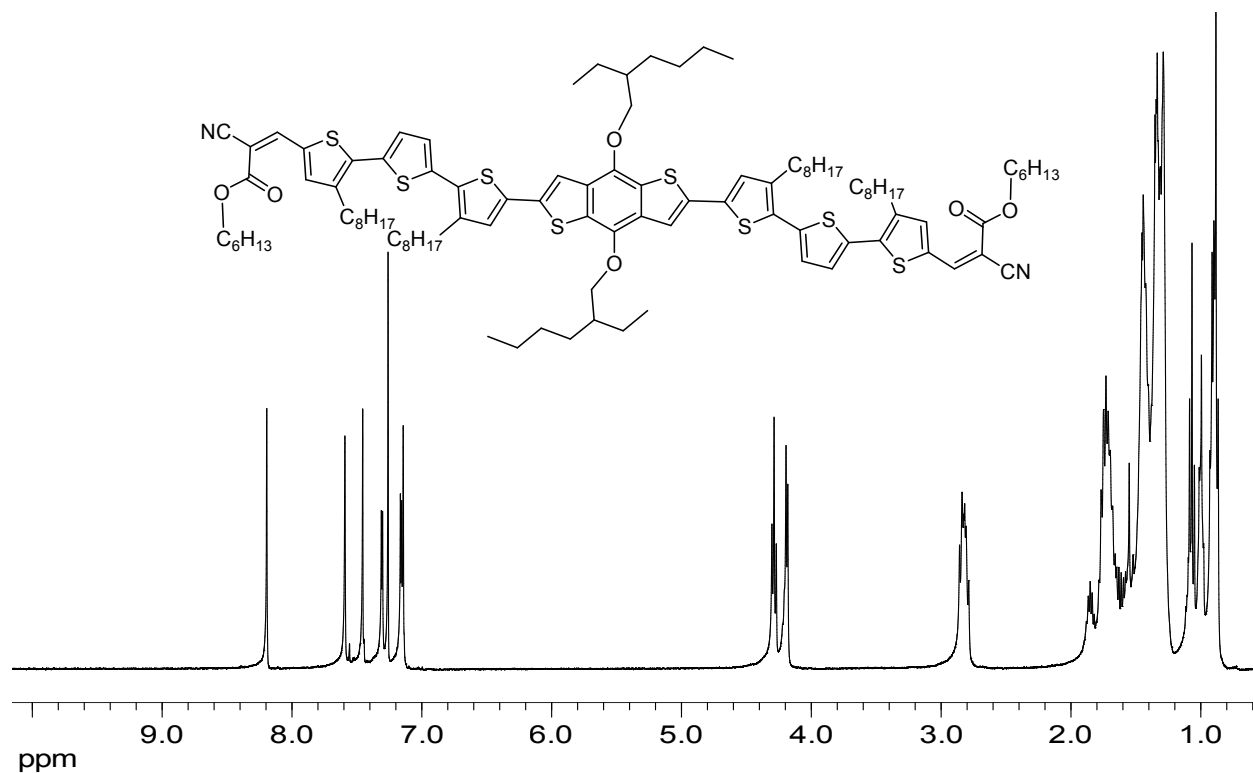


Figure S10. ^1H NMR spectrum of $\text{BDT}(\text{T}_3\text{A})_2$ (600 MHz).

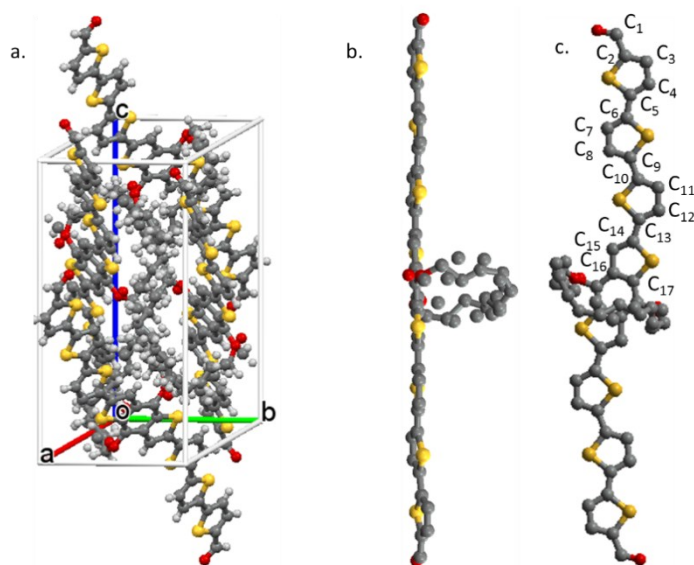


Figure S11. The unit cell of $\text{RingBDT}(\text{T}_3\text{CHO})_2$ and the side and top views of the molecule. There is some fuzziness in the positions of atoms of the protection ring.

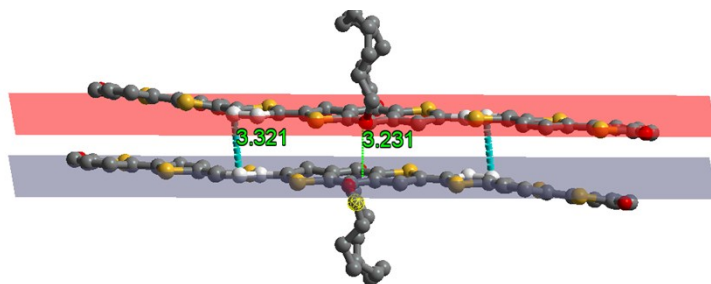


Figure S12. RingBDT(T₃CHO)₂ dimer in single crystal. Shortest contacts (with a distance of 3.321 Å) are between carbon atoms in the thiophene units bonded to BDT. The shortest interplanar distance is between the planes (gray and red) defined by the four white-color carbon atoms in each molecule.

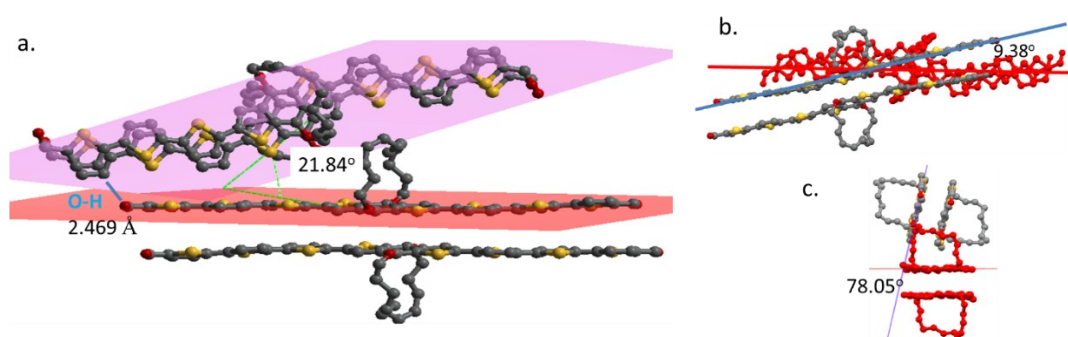


Figure S13. The side (a), top (b) and end (c) views of two sets of stacked dimers. In the side view, the red plane is the mean average plane of the π -backbone, and the violet plane is defined by the four terminal carbon atoms of the four terminal thiophene units in the top dimer. In b and c, the bottom dimer is colored in red.

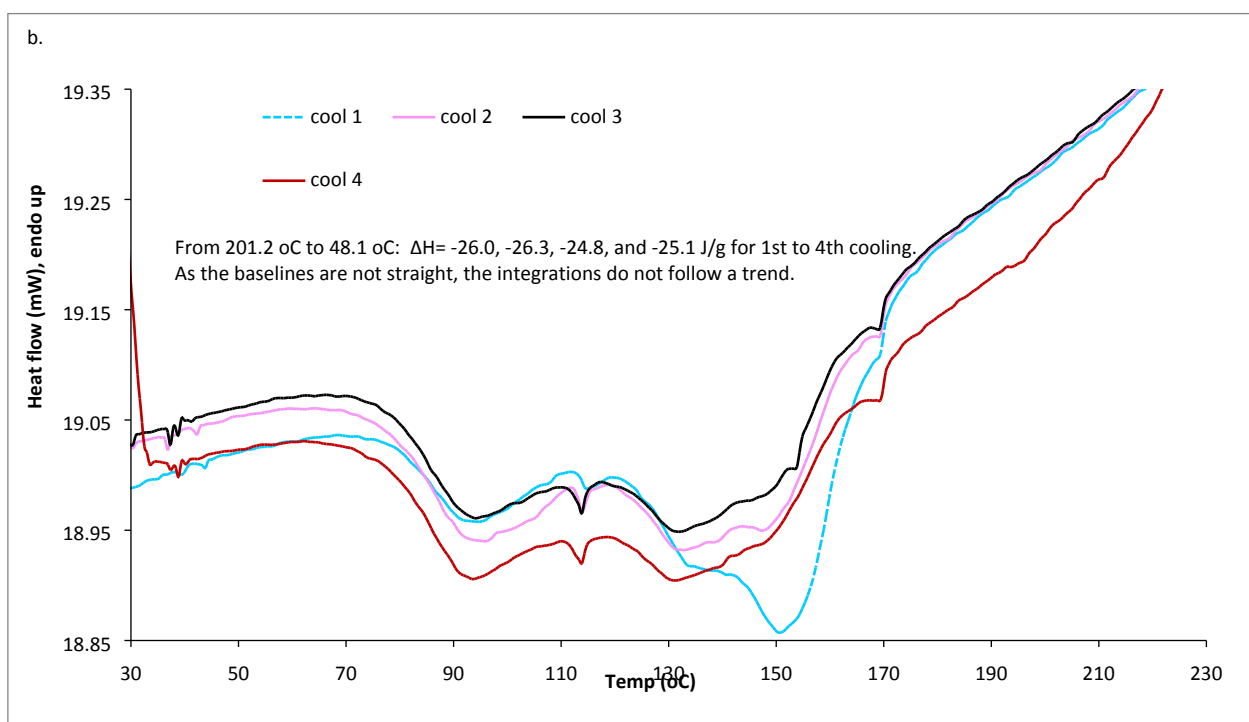
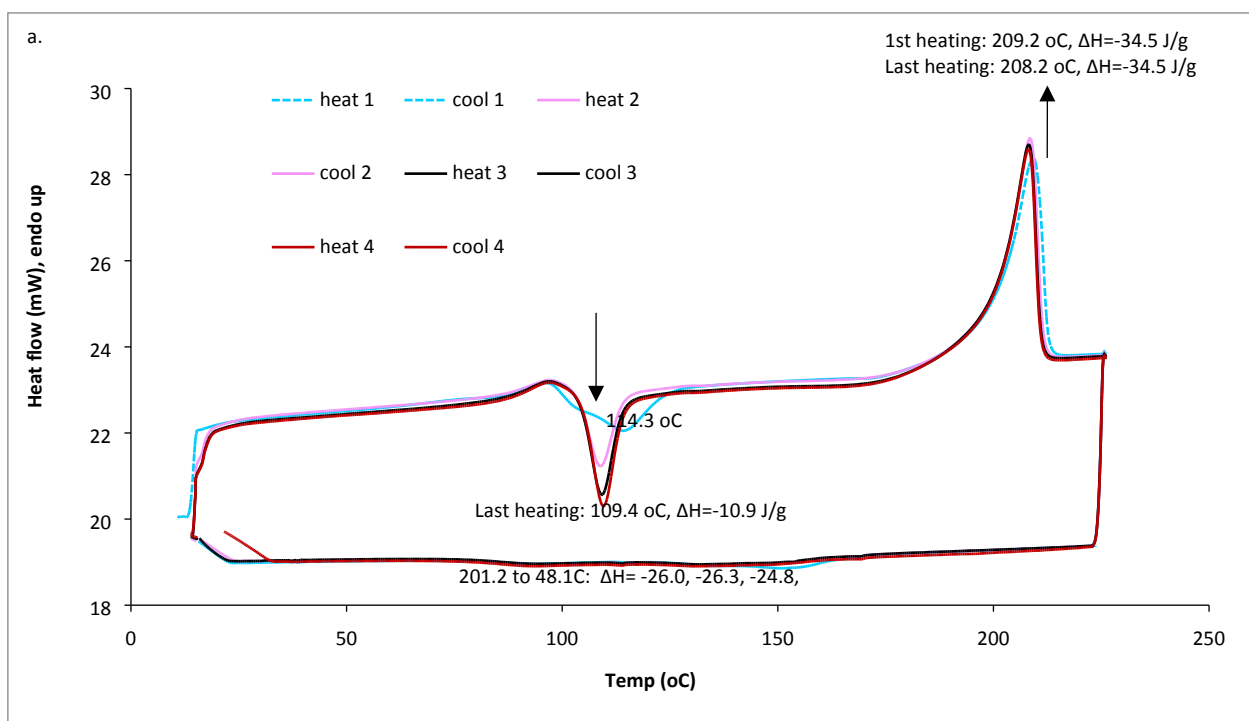


Figure S14. a) A four-cycle DSC scan of RingBDT(T_3A). Mass of sample: 8.4 mg. The heating rate was 10 °C/min, and the cooling rate was 5 10 °C/min. b) A magnified view of the cooling scans.

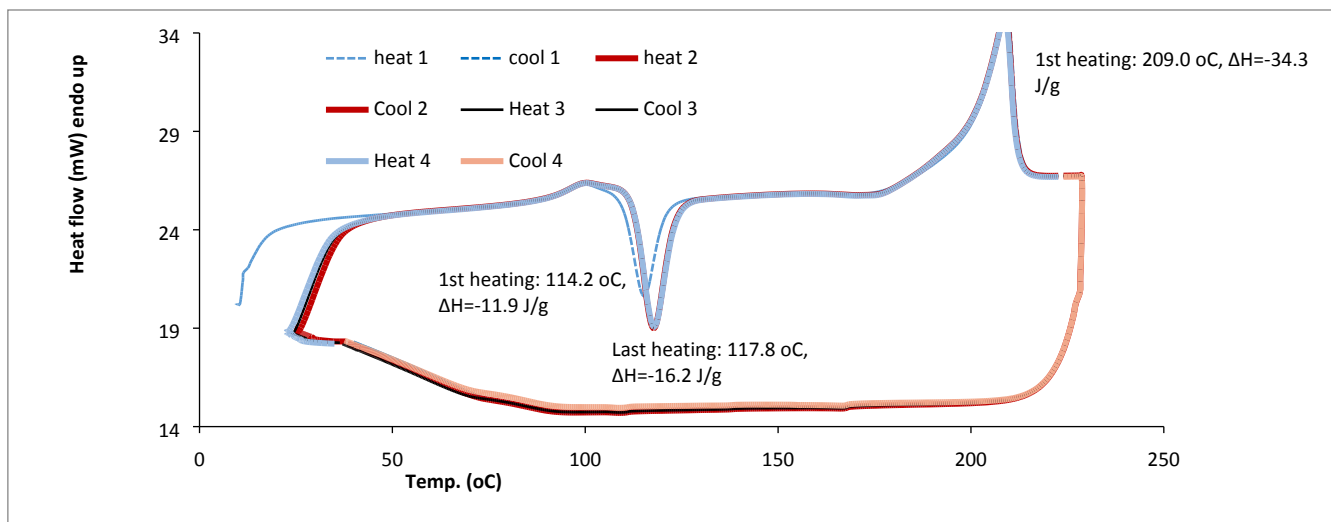


Figure S15. A four-cycle DSC scan of RingBDT(T₃A) at a higher heating and cooling rate of 20 °C/min. The Fig. S14 sample was reused. Three significant digits are used for enthalpy changes to allow comparison between different cycles. The intensity of the crystallization peak on the second and later heating sweeps are same and closer to the melting peak, indicating that crystallization upon cooling became even slower when the cooling rate was increased.

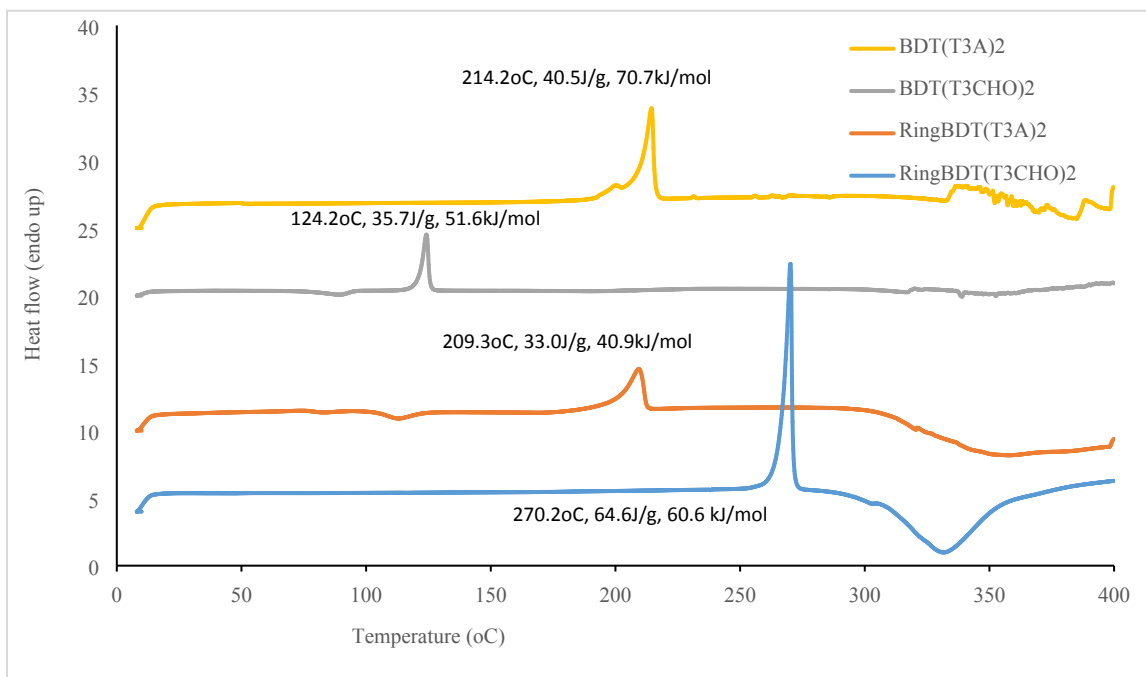


Figure S16. DSC thermograms of RingBDT(T₃CHO)₂, RingBDT(T₃A)₂, BDT(T₃CHO)₂, and BDT(T₃A)₂. N₂ flow rate: 20 mL/min. Heating rate: 10 °C/min.

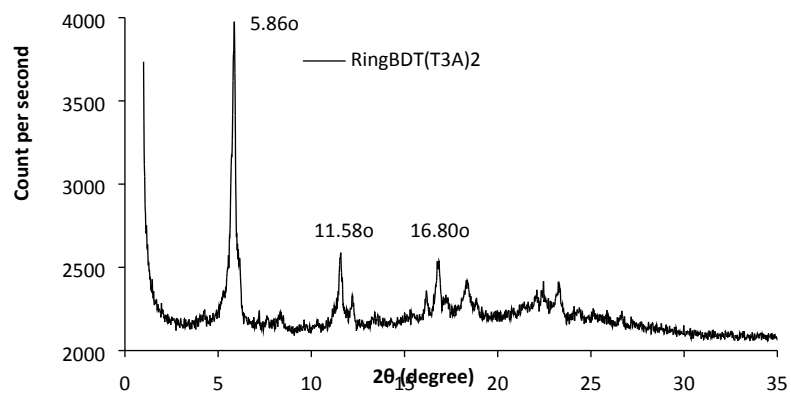


Figure S17. Powder X-ray diffractogram of RingBDT(T₃A)₂.

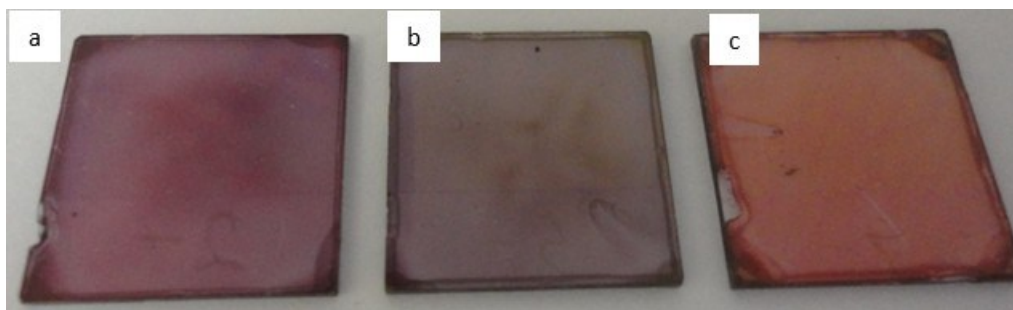


Figure S18. Optical images of a BDT(T₃A)₂ films spin-coated from chloroform (a) and chlorobenzene (b) solutions, and a RingBDT(T₃A)₂ film spin-coated from chlorobenzene solution (c) at 1000 rpm.

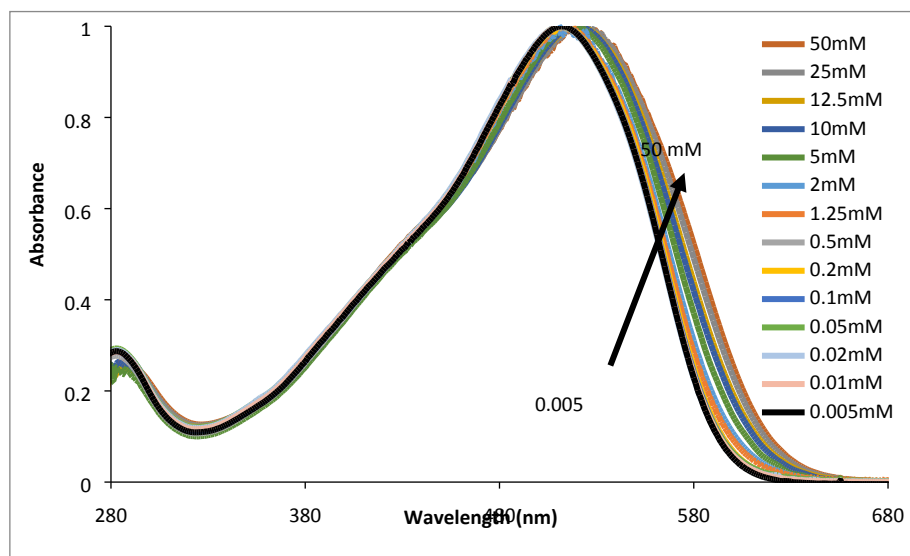


Figure S19. UV-vis absorption spectra of RingBDT(T₃A)₂ chloroform solutions of different concentrations.

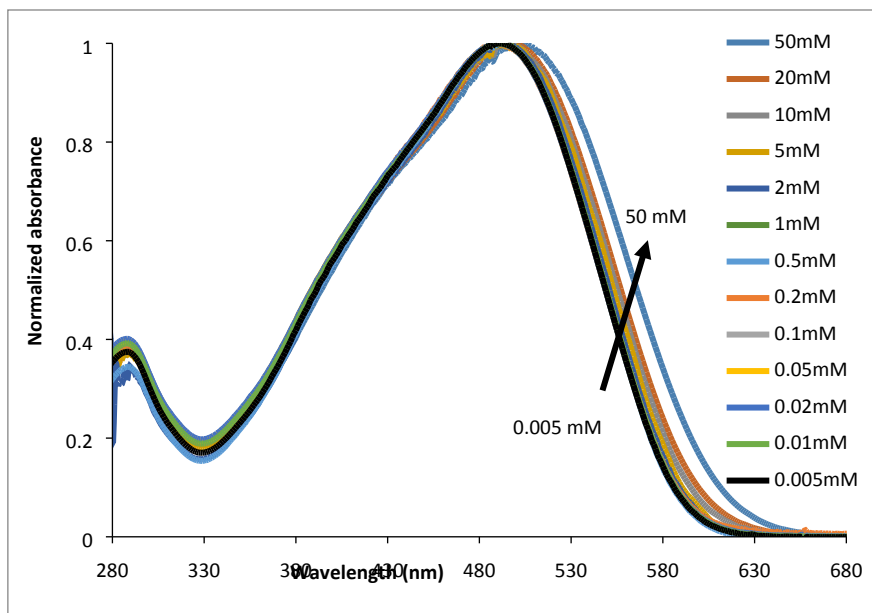


Figure S20. UV-vis absorption spectra of $\text{BDT}(\text{T}_3\text{A})_2$ chloroform solutions of different concentrations.

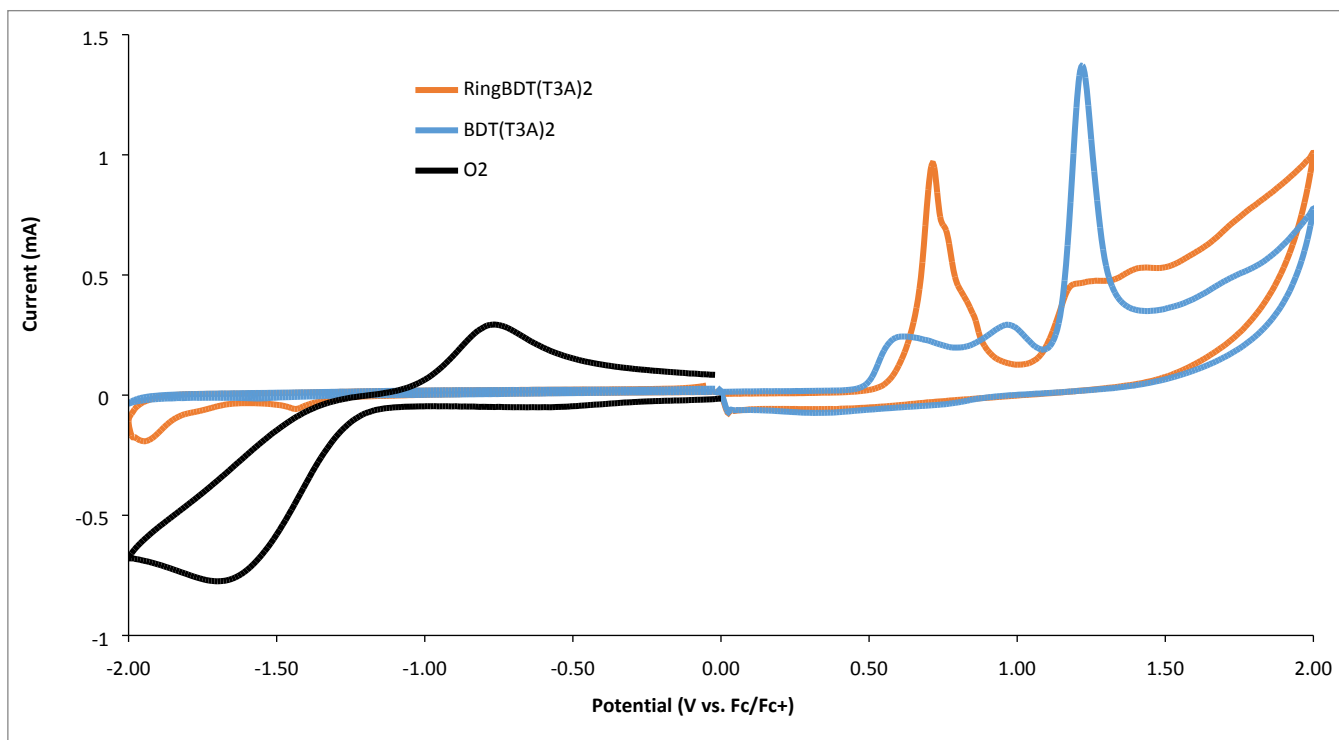


Figure S21. Cyclic voltammograms of $\text{RingBDT}(\text{T}_3\text{A})_2$ and $\text{BDT}(\text{T}_3\text{A})_2$ over a potential range of -2 V to 2 V, and dissolved oxygen. In the CV experiment of oxygen, the electrolyte solution was not purged at all. $\text{RingBDT}(\text{T}_3\text{A})_2$ was dissolved when the potential reached +2 V, while $\text{BDT}(\text{T}_3\text{A})_2$ stayed on the electrode at all time.

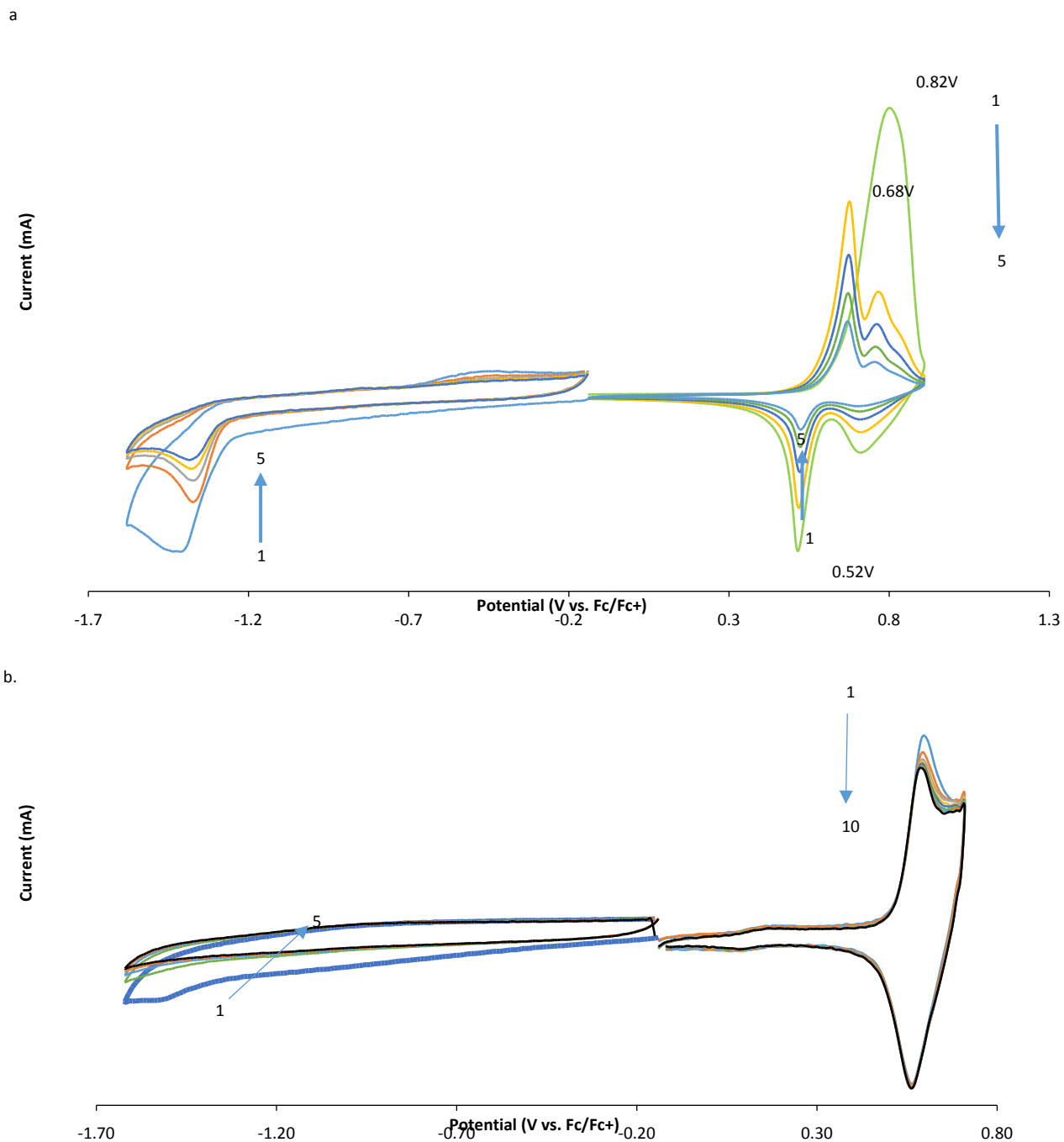


Figure S22. Cyclic voltammograms of RingBDT(T_3A)₂ (a) and BDT(T_3A)₂ (b) thicker films. The currents of the negative scans are very small, and are scaled up by 6 times for a better view. Reference electrode: Ag/AgNO₃. The chromophore coatings on the Pt wire working electrode are thicker than those used in Fig. 9a&b.

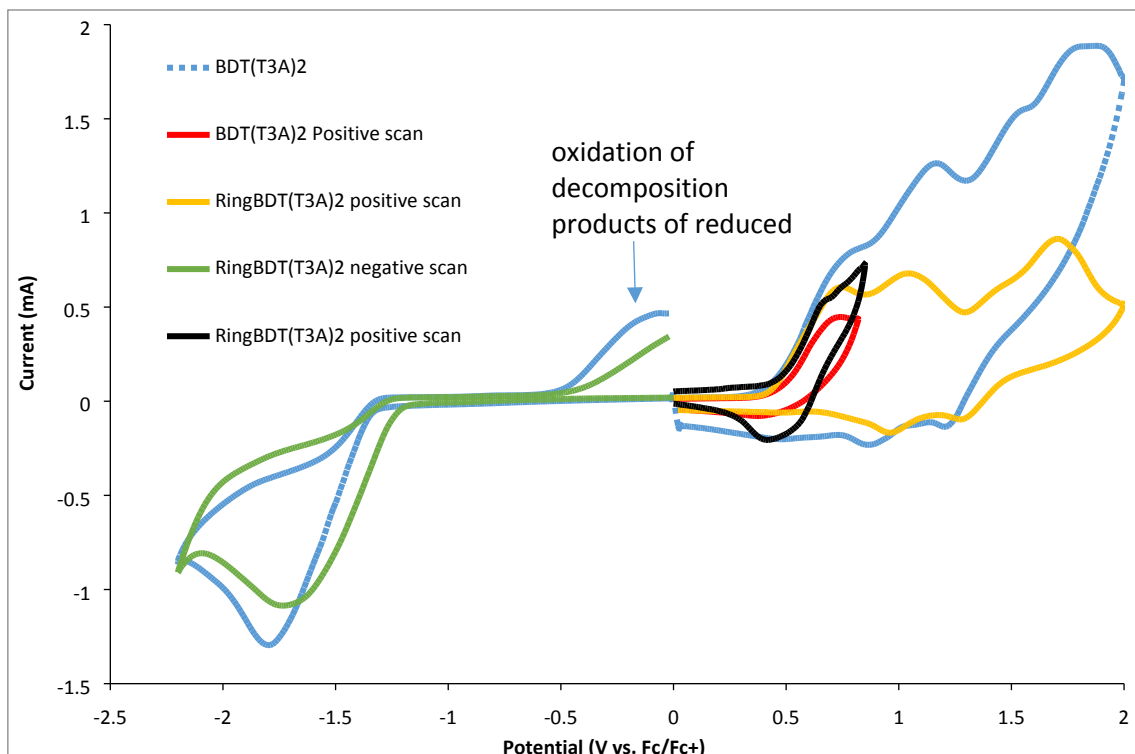


Figure S23. Cyclic voltammograms of RingBDT(T₃A)₂ and BDT(T₃A)₂ solutions. Reference electrode: Ag/AgNO₃ in 0.1M TBA HFP/MeCN. The electrolyte solution in the cell is 0.1M TBA HFP in dichloromethane. Chromophore was coated on a Pt wire working electrode. CV scan was started immediately after the working electrode was inserted in the cell. Chromophore was dissolved immediately, forming a solution around the working electrode.

	$E_{red/ox}^b$ (V)	LUMO/HOMO (eV)	E_g^{EC} (eV)
RingBDT(T ₃ A) ₂	-1.23/0.42	-3.77/-5.52	1.65
BDT(T ₃ A) ₂	-1.34/0.44	-3.76/-5.54	1.78

Table S1. Performance of inverted solar cells of BDT(T₃A)₂:PC₆₀BM (as deposited)

	V_{oc}	J_{sc}	FF	Efficiency
Batch 1 - Cell 1	0.83	4.48	0.67	2.48
Batch 1 - Cell 2	0.85	4.49	0.64	2.46
Batch 1 - Cell 3	0.84	4.12	0.61	2.11
Batch 1 - Cell 4	0.82	4.18	0.55	1.90
Batch 1 - Cell 5	0.86	4.07	0.61	2.12
Batch 2 - Cell 1	0.89	4.25	0.58	2.19
Batch 2 - Cell 2	0.89	4.32	0.59	2.27
Batch 2 - Cell 3	0.85	3.71	0.62	1.95
Batch 2 - Cell 4	0.86	4.65	0.63	2.54
Batch 2 - Cell 5	0.87	4.26	0.65	2.40
Batch 2 - Cell 6	0.88	3.91	0.62	2.14
				2.23 - Average

Table S2. Performance of inverted solar cells of BDT(T₃A)₂:PC₆₀BM (annealed on a 100 °C hot plate for 10 minutes)

	V_{oc}	J_{sc}	FF	Efficiency
Cell-1	0.68	1.21	0.36	0.30

Cell-2	0.85	0.94	0.49	0.39
Cell-3	0.82	1.19	0.48	0.47
				0.38 - Average

Table S3. Performance of inverted solar cells of RingBDT(T₃A)₂:PC₆₀BM (as deposited, no DIO)

	Voc	Jsc	FF	Efficiency
Cell-1	0.85	4.85	0.35	1.45
Cell-2	0.85	4.61	0.35	1.39
Cell-3	0.83	5.25	0.35	1.52
Cell-4	0.85	4.51	0.40	1.52
Cell-5	0.82	5.01	0.37	1.52
Cell-6	0.87	5.01	0.35	1.53
				1.49 - Average

Table S4. Performance of inverted solar cells of RingBDT(T₃A)₂:PC₆₀BM (as-cast with DIO)

	Voc	Jsc	FF	Efficiency
Cell-1	0.87	5.87	0.42	2.12
Cell-2	0.88	6.01	0.40	2.12
Cell-3	0.92	5.36	0.42	2.07
Cell-4	0.90	5.55	0.43	2.13
Cell-5	0.88	6.19	0.42	2.30
Cell-6	0.88	6.19	0.43	2.35
				2.18 - Average

Table S5. Performance of inverted solar cells of RingBDT(T₃A)₂:PC₆₀BM (with DIO, annealed on a 100 °C hot plate for 10 minutes)

	Voc	Jsc	FF	Efficiency
Batch 1 - Cell 1	0.92	5.35	0.44	2.18
Batch 1 - Cell 2	0.86	5.82	0.49	2.46
Batch 1 - Cell 3	0.91	5.57	0.47	2.39
Batch 1 - Cell 4	0.88	5.56	0.48	2.34
Batch 1 - Cell 5	0.87	4.97	0.48	2.07
Batch 2 - Cell 1	0.88	6.19	0.43	2.35
Batch 2 - Cell 2	0.90	5.55	0.44	2.17
Batch 2 - Cell 3	0.89	6.01	0.40	2.16
Batch 2 - Cell 4	0.88	5.87	0.42	2.16
Batch 2 - Cell 5	0.84	5.66	0.44	2.10
				2.24 - Average

Table S6. RingBDT(T₃A)₂ devices performances of devices in a normal device configuration: Glass/ITO/PEDOT-PSS/donor:PC₆₀BM/Ca/Al. RingBDT(T₃A)₂:PC₆₀BM = 1:1 wt, 15mg:15mg in 1mL o-dichlorobenzene.

Spin condition	J _{sc} (mA/cm ²)	V _{oc} (V)	FF (%)	Eff. (%)
1000 rpm for 30s	4.69	0.95	31.2	1.78

1600 rpm for 30s	5.49	0.96	33.8	1.78
2400 rpm for 30s	6.08	0.97	36.4	2.15
2600 rpm for 30s	5.95	0.96	34.7	1.98

Table S7. BDT(T_3A)₂ devices performances of devices in a normal device configuration. BDT(T_3A)₂:PC₆₀BM = 8mg:4mg in 1 ml CHCl₃. Spin rate: 1700 rpm. Ramp time: 1s.

	V_{oc} (V)	J_{sc} (mA/cm ²)	FF	Eff. (%)
CHCl ₃ only	0.79	2.67	0.30	0.63
CHCl ₃ with CB (0.2 wt%)	0.74	0.15	0.134	0.015
CHCl ₃ with CB (0.83 wt%)	0.68	0.005	0.166	0.0006

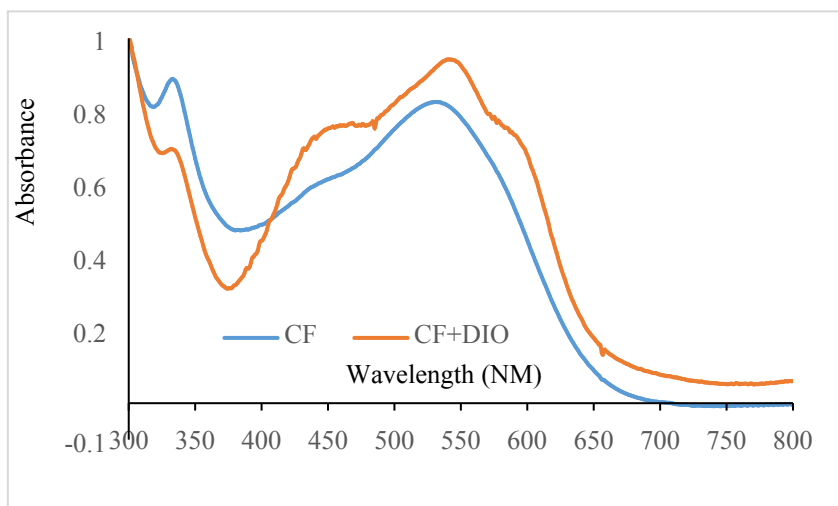


Figure S24. The absorption spectra of RingBDT(T_3A)₂:PC₆₀BM films processed without and with DIO.